

# Integrated Multi-Level Control Value and Variation Trend Early-Warning Approach for Deformation Safety of Arch Dam

Huaizhi Su<sup>1,2</sup> · Xiaoqun Yan<sup>2</sup> · Hongping Liu<sup>3</sup> ·  
Zhiping Wen<sup>4</sup>

Received: 24 August 2016 / Accepted: 16 March 2017 /  
Published online: 24 March 2017  
© Springer Science+Business Media Dordrecht 2017

**Abstract** Appropriate early-warning index of dam deformation can be used to identify the structural behavior in real time. It is an important measures to monitor the service safety of dam engineering. This paper focuses on the approach determining the early-warning index of arch dam deformation by analyzing the prototypical observations of dam safety and implementing the numerical simulation of dam structure. First, according to the long-term deformation process of arch dam, an early-warning criterion, which combines the multi-level control value and variation trend of dam deformation, is presented. Second, the numerical analysis for structural failure is implemented to calculate the global safety factor of arch dam. A method determining the global safety factor-based control value of dam deformation is developed. Third, the multi-resolution analysis of wavelet is introduced to identify the variation trend of dam deformation from the measured data. The variation trend rule is given to judge the deformation status of arch dam. Finally, the deformation behavior of one actual arch dam is taken as an example. The multi-level control value formula of dam deformation is given. It is combined with the variation trend of dam deformation to fulfill the comprehensive evaluation of deformation safety. It is indicated that the proposed approach is suitable to be used to determine the early-warning index of arch dam deformation, can help with identifying the service safety and potential risk of dam engineering.

---

✉ Huaizhi Su  
su\_huaizhi@hhu.edu.cn

<sup>1</sup> State Key Laboratory of Hydrology-Water Resources and Hydraulic Engineering, Hohai University, Nanjing 210098, China

<sup>2</sup> College of Water Conservancy and Hydropower Engineering, Hohai University, Nanjing 210098, China

<sup>3</sup> National Engineering Research Center of Water Resources Efficient Utilization and Engineering Safety, Hohai University, Nanjing 210098, China

<sup>4</sup> Department of Computer Engineering, Nanjing Institute of Technology, Nanjing 211167, China

**Keywords** Arch dam · Deformation safety · Early-warning index · Control value · Variation trend

## 1 Introduction

Under the long-term action of dynamic and static cyclic loads, material aging, environmental factors, the dam structural behavior such as deformation and stress will change, and even the structural failure can be caused. To diagnose the safety status in real time and adopt the appropriate operation mode, the early-warning index of structural behavior is often applied to the dam management (Hossain 2010; Wu et al. 2011; Zhong et al. 2011). It can play an important role in ensuring the service safety of dam engineering. Dam body and dam foundation are regarded as a dam system. The parameters and corresponding criterion, which are suitable to describe the safety status of dam system, need to be selected to determine the early-warning index. At present, the control value of structural response, which can be determined by analyzing the prototypical observations of dam safety, implementing the numerical calculation or physical experiment of dam structure, is usually taken to monitor the dam safety (Lei et al. 2011). The variation trend of structural response can also be applied to the structural behavior identification (Stojanovic et al. 2013).

The control value of dam deformation can be regarded as an index distinguishing the different working status of dam structure, such as normal, abnormal, dangerous or damaged (Kao and Loh 2013; Mata et al. 2014). According to the prototypical observations of dam safety and the numerical calculations of dam structure, the deformation control values of dam body and dam foundation can be determined using the confidence interval method, the little probability method and the limit state method (Wu and Su 2005; Lei et al. 2011; Wu et al. 2011; Su et al. 2012). The confidence interval method is the most commonly used to determine the control values of dam deformation by building the statistical relationship models between dam deformation and long-term loads. However it has the following shortcomings. If the statistical relationship model is built using the observation sequence without undergoing the most unfavorable load combination, it can only forecast more accurately the deformation response within the ever experienced loads. So the determined control value of dam deformation cannot be used to judge the deformation status under some unfavorable loads. Furthermore, the standard deviations of calculated results and the confidence intervals, which correspond with the different modeling data series, are different. If the standard deviation is larger, the control value determined using the confidence interval method may exceed the actual deformation extremum, and even the omissive judgment may be caused. The little probability method can estimate the control values of dam deformation with the representative data which are selected from all prototypical observations by considering the unfavorable load combination on the strength and stability of dam system. However, only if there is a long observed data series and the dam has undergone the more unfavorable load combinations, the control value can approach to the deformation extremum. According to the limit equilibrium conditions of dam safety by calculating the structural resistance and critical load combination, the limit state method can be adopted to estimate the control values of dam deformation. Due to little change of structural resistance of one dam, the load and its response should be controlled to ensure the dam safety. Gravity dam is mainly affected by water load. Its most unfavorable load can easily be determined. It is difficult to give the most unfavorable

load combination of arch dam. Generally, a great deal of trial calculations need to be fulfilled to obtain the reasonable results. Above methods are directly or indirectly relevant to statistics theory.

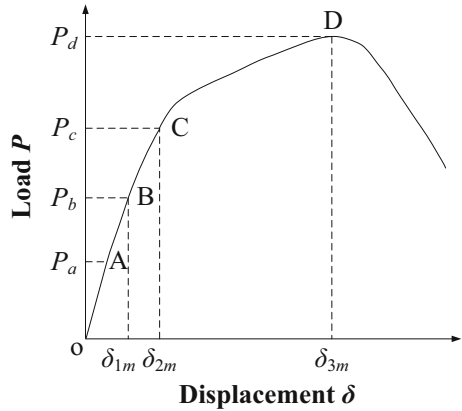
Trend component of structural response is often taken as a state parameter describing the safety status of dam body-foundation system. The observed data of structural response can be regarded as a digital signal series composed of different frequencies. Some time-frequency analysis approaches such as digital filtering technique and support vector machine can be used to extract the trend component from observed data (Ardito et al. 2008; Cheng and Zheng 2013; Ranković et al. 2014; Su et al. 2015). The digital filtering technique based on Fourier transform can analyze the signal with periodic or stationary variation. However the prototypical observed data series of dam safety is often non-stationary. So the digital filtering technique has certain limitations in extracting the trend component of structural response. As a time-frequency analysis method of nonlinear and non-stationary time series, the wavelet analysis method has the potential to extract effectively the trend component of dam structural response, especially by implementing the multi-resolution analysis of wavelet.

Due to the variation of own structure, the uncertainty of load and environment, and the complexity of causal link between internal and external influence factors, the great difficulty is brought in determining the early-warning index of arch dam deformation. This paper takes an arch dam system composed of dam body and dam foundation as research object. In Section 2, the long-term deformation process of arch dam is analyzed. The deformation trend component is taken as a state parameter describing the safety status of arch dam system. The early-warning criterion on deformation safety, which combines the multi-level control value and trend component of dam deformation, is investigated. The methods determining the multi-level control values of dam deformation and extracting the trend component of dam deformation are presented in Section 3 and Section 4, respectively. An actual arch dam is taken as an example in Section 5. According to the prototypical observations of dam safety and the numerical calculations of dam structure, the early-warning index of dam deformation is determined using the proposed approach. The safety status of dam deformation is evaluated.

## 2 Integrated Early-Warning Criterion on Deformation Safety of Arch Dam

The deformation of arch dam, which is affected by internal and external factors, has strong nonlinear characteristics. The internal factors include the concrete aging of dam body and the rock creep of dam foundation that make the mechanical properties of dam material be changed and cause the structural deformation of arch dam. The external factors, such as extraordinary flood, earthquake, sudden temperature rise or drop, can lead to the abnormal changes of arch dam deformation. The long-term deformation process of arch dam as a high-order statically indeterminate structure is extremely complex. According to a large number of engineering experience and experimental results, it has been known that the progressive failure process of arch dam can be divided into the linear elastic phase, the quasi linear elastic phase, the yield deformation phase and the failure phase, as shown in Fig. 1.

**Fig. 1** Load-displacement curve of arch dam



- (1) Linear elastic phase. If the stresses at any location in arch dam body under the load  $P(t)$ , even the tensile stresses in dam heel zone, are not more than the proportional limit of material strength, the dam body is in a perfect elastic state and the stress-strain relationship is linear. As the phase OA shown in Fig. 1, the relationship between the load  $P(t)$  and the displacement  $\delta(t)$  is generally linear elastic or viscoelastic.
- (2) Quasi linear elastic phase. With the increase of the load  $P(t)$ , some cracks appear in the dam heel zone or the upstream arch abutment. The downstream compressive stress will increase after the stress redistribution. When the load increases to  $P_b$ , the compressive stress in dam toe zone reaches the strength limit, usually the proportional limit of material strength. The arch dam is in a quasi linear elastic state and its deformation process is similar to the phase AB shown in Fig. 1. The relationship between the load  $P(t)$  and the displacement  $\delta(t)$  is generally linear.

When the arch dam is in the linear elastic or quasi linear elastic phase, the relationship between the load  $P(t)$  and the displacement  $\delta(t)$  of dam body and dam foundation is linear elastic in general, as the phase OB shown in Fig. 1. The deformation threshold  $\delta_{1m}$ , which corresponds to the linear elastic and quasi linear elastic phases, is addressed as the first-level control value.

- (3) Yield deformation phase. With the further increase of the load  $P(t)$  or the change of parameters, the downstream compressive stress of arch dam will increase, the crack zone will expand and the arch dam is in a yield state. As the phase BC shown in Fig. 1, the structural deformation increases by a large margin, the relationship between the load  $P(t)$  and the displacement  $\delta(t)$  is nonlinear. The arch dam is in an elastoplastic or visco-elastoplastic state with small deformation. The corresponding deformation threshold  $\delta_{2m}$  is addressed as the second-level control value.
- (4) Failure phase. After the load  $P(t)$  increases continuously to a certain value or the parameter exceeds one limit, the deformation of arch dam may increase rapidly. The zones of crack, yield and compression failure will expand quickly. The arch dam presents the large deformation state. When the load reaches the critical value, the arch dam will lose the load-bearing capacity and be totally destroyed. As the phase CD shown in Fig. 1, the arch dam is in a visco-elastoplastic state with large deformation. The corresponding deformation threshold  $\delta_{3m}$  is addressed as the third-level control value. In practice, the arch dam is not permitted in the failure phase.

The structural behavior of arch dam can be described with three phases, namely the linear elastic or quasi linear elastic phase, the elastoplastic phase and instability failure phase. The service safety of arch dam can be expressed with the normal, abnormal or dangerous status. Correspondingly, the three levels are adopted to implement the early-warning of dam deformation. The early-warning criterion on deformation safety of arch dam can be expressed as follows.

If the dam deformation  $\delta_m$  and its trend component  $\delta_\theta$  satisfy the condition as Eq. (1), the arch dam is in an elastoplastic or visco-elastoplastic phase. Furthermore, some hidden dangers are detected. Then the dam deformation is abnormal. The arch dam should be in the first-level early-warning state.

$$\delta_{1m} \leq \delta_m < \delta_{2m}, \frac{d^2 \delta_\theta}{dt^2} = 0 \quad (1)$$

where  $\delta_m$  represents the observed or forecasted value of horizontal displacement at dam crest or dam foundation of key dam section;  $\delta_{1m}$  is the first-level control value of dam deformation, which can be determined by numerical calculation with viscoelastic model;  $\delta_{2m}$  is the second-level control value of dam deformation, which can be determined by numerical calculation with visco-elastoplastic model of small deformation;  $\delta_\theta$  denotes the trend component of dam deformation;  $t$  is time.

If the dam deformation  $\delta_m$  and its trend component  $\delta_\theta$  satisfy the condition as Eq. (2), the arch dam is in a plastic or visco-plastic phase. Furthermore, some hidden dangers are detected. Then the dam deformation is dangerous. The arch dam should be in the second-level early-warning state.

$$\delta_{2m} \leq \delta_m < \delta_{3m}, \frac{d^2 \delta_\theta}{dt^2} > 0, \frac{d^3 \delta_\theta}{dt^3} < 0 \quad (2)$$

where  $\delta_{3m}$  is the third-level control value of dam deformation, which can be determined by numerical calculation with visco-elastoplastic model of large deformation.

If the dam deformation  $\delta_m$  and its trend component  $\delta_\theta$  satisfy the condition as Eq. (3), the arch dam is in a failure phase with large deformation. The arch dam should be in the third-level early-warning state.

$$\delta_m = \delta_{3m}, \frac{d^3 \delta_\theta}{dt^3} = 0 \quad (3)$$

It can be seen from Eqs. (1–3) that the deformation safety of arch dam can be identified by integrating two early-warning indices, namely control value and variation trend of dam deformation.

### 3 Control Value–Based Early-Warning Index on Deformation Safety of Arch Dam

The deformation control values with three levels correspond to the linear elastic, elastoplastic and instability failure phases of arch dam. So the finite element method (FEM) can be adopted to implement the viscoelastic calculation, the visco-elastoplastic calculation of small deformation and large deformation. The strength, stability and

crack are regarded as constraint conditions. The calculated deformations, which satisfy the limit state equations of above three phases, are the deformation control values with three levels.

When the first-level control value  $\delta_{1m}$  of dam deformation is determined, the strength and stability conditions of arch dam should be satisfied under the design load combination. So the first-level control value  $\delta_{1m}$  of dam deformation can be expressed as follows.

$$\delta_{1m} = F\left(\sigma_{et} \leq [\sigma]_e, \sigma_{st} \leq [\sigma]_s, K = \frac{R}{S} \geq [K]\right) \quad (4)$$

where  $[\sigma]_e$  and  $[\sigma]_s$  are the allowable tensile and compressive stresses;  $\sigma_{et}$  and  $\sigma_{st}$  are the actual tensile and compressive stresses;  $K$  represents the actual stability safety factor;  $[K]$  is the allowable safety factor;  $R$  and  $S$  are the anti-sliding force and the sliding force.  $K = R/S = (f \sum F + cA) / \sum P$ ,  $c$  and  $f$  are the cohesion and the friction coefficient,  $\sum F$  and  $\sum P$  are the normal stress and the tangential stress of sliding surface which are caused by all loads acting on dam body,  $A$  is the contact area. When the anti-sliding force  $R$  is calculated, the parameters  $c$  and  $f$  are the mean of small peak values obtained through test-in-place. The design load combination is adopted to calculate the sliding force  $S$ .

When the second-level control value  $\delta_{2m}$  of dam deformation is determined, the following constraint conditions of arch dam should be satisfied. The strength condition is  $\sigma_{et} \leq \sigma_e$ ,  $\sigma_{st} \leq \sigma_s$ . The stability condition is  $R \geq S$ . The crack condition is  $K_c \geq K_\sigma$ . So the second-level control value  $\delta_{2m}$  of dam deformation can be expressed as follows.

$$\delta_{2m} = F(\sigma_{et} \leq \sigma_e, \sigma_{st} \leq \sigma_s, R \geq S, K_c \geq K_\sigma) \quad (5)$$

where  $\sigma_e$  and  $\sigma_s$  are the yield strengths of tensile and compressive stresses;  $K_\sigma$  is the stress intensity factor;  $K_c$  is the fracture toughness. When the anti-sliding force  $R$  is calculated, the parameters  $c$  and  $f$  are the yield values obtained through test-in-place. The most unfavorable load case, which causes the cracks, is adopted to calculate the sliding force  $S$ .

When the third-level control value  $\delta_{3m}$  of dam deformation is determined, the following constraint conditions of arch dam should be satisfied. The strength condition is  $\sigma_{et} \leq \sigma_{el}$ ,  $\sigma_{st} \leq \sigma_{sl}$ . The stability condition is  $R \geq S$ . So the third-level control value  $\delta_{3m}$  of dam deformation can be expressed as follows.

$$\delta_{3m} = F(\sigma_{et} \leq \sigma_{el}, \sigma_{st} \leq \sigma_{sl}, R \geq S) \quad (6)$$

where  $\sigma_{el}$  and  $\sigma_{sl}$  are the ultimate tensile strength and the ultimate compressive strength. When the anti-sliding force  $R$  is calculated, the parameters  $c$  and  $f$  are the mean of peak values obtained through test-in-place. The ultimate load combination with small appearance probability should be adopted to calculate the sliding force  $S$ .

Since arch dam is a high-order statically indeterminate structure, it is difficult to avoid the local yield during long-term service. However, arch dam can still work normally as long as the damage is not serious enough to affect the global safety of dam body-foundation system. According to the rules as Eqs. (4–6) determining the control values of dam deformation and the long-term deformation characteristics as shown in Fig. 1, the control values of dam deformation may be related to the failure modes of arch dam. By calculating the global safety factors corresponding to the failure modes of arch dam, the deformation control values with three levels can be determined.

The global safety of arch dam can be described with the following indices such as the safety factor obtained by the strength reduction or overload way, the point safety factor and the reliability index (Sujathea and Chandra Kishen 2003; Yenigun and Erkek 2007; Huang and Jia 2009; Jin et al. 2011; Lin et al. 2014). In this paper, the strength reduction-based safety factor is taken. The numerical simulation is implemented to analyze the structural behavior with the adjusted strength parameters. Under the action of constant loads, the rock parameters of dam foundation, such as cohesion and inner friction angle, are reduced gradually in proportion. The reduction coefficient  $K$  corresponding to arch dam instability represents the stability safety factor of arch dam. The strength reduction-based approach can consider the uncertainty and weakening effect of material strength, and can describe the instability process of arch dam. The following conventional criteria can be adopted to identify the stability of arch dam using the strength reduction-based FEM.

- (1) Convergence criterion. The strength-type instability is a failure process with the extreme points. Its load-displacement curve has some extreme points, as shown in Fig. 1. From the calculation point of view, the iterative solving process cannot converge. The convergence criterion is more easy and convenience to judge the structural failure. But in the practical calculations, the difference of calculated safety factors may be caused by the finite element mesh form and calculation accuracy.
- (2) Run-through criterion of plastic zone. The yield zones are extended, connected, and finally a run-through yield region is formed, the structure loses the load-bearing capacity. The numerical calculation is implemented to observe the change and distribution of plastic zones with the strength reduction coefficient. When the increase of reduction coefficient makes a run-through plastic region emerge, the instability failure is caused. This instability criterion has a problem on the strain control standard. The larger strain control value may make the actual instability state be mistaken for the stability state or the limit equilibrium state.
- (3) Displacement jump criterion. According to the displacement of characteristic points in calculation domain, the structural behavior is identified. If a mutation of calculated displacement occurs, namely the displacement-reduction coefficient curve has a breaking point, the instability failure is caused. The corresponding strength reduction coefficient at this time can be regarded as the safety factor of arch dam.

The run-through plastic region formation of structural planes is only the inevitable result of arch dam failure, but not sufficient and necessary condition. So in this paper, the plastic zone run-through criterion of structural planes and the displacement jump criterion of characteristic points are combined to identify the stability safety of arch dam. When the strength reduction coefficient is small, the maximal displacements at the crown cantilever crest, the dam bottom and the dam body increase linearly with the reduction coefficient. It indicates that the whole arch dam is in an elastic working state. With the successive increase of reduction coefficient, the radial displacement increases further and it shows the nonlinear change characteristics. The displacement growth rises also. The dam enters the yield deformation stage. When the run-through plastic region of structural planes is formed, the arch dam can be considered to be completely yielded. If the reduction coefficient increases further, the arch dam will lose the load-bearing capacity and the numerical calculation is not convergent. This moment means the failure of arch dam.

## 4 Variation Trend–Based Early-Warning Index on Deformation Safety of Arch Dam

The variation trend of arch dam deformation reflects the irreversible deformation caused by the creep of concrete and rock, the faults and joints in the rock mass, other hidden dangers. For an arch dam with normal structural behavior, its trend component will change rapidly in the initial impoundment period or in one or two years after some engineering measures implementation. And then it will become stable gradually as the time goes by. A sudden increase or great change in the trend component of dam deformation means that the critical situations of arch dam may occur. So the variation of trend component can be used to identify the deformation safety of arch dam. The statistical analysis methods can be adopted to extract the trend component of arch dam deformation. However, if the trend component is closely related to its influence factors, this relevance will have a great effect on the extracted results (Su et al. 2011). The observations of dam deformation can be regarded as a digital signal series composed of different frequencies. In this paper, according to the frequency characteristics of random component, periodic component and trend component, the wavelet analysis method is introduced to implement the decomposition of observed deformation data series. The deformation safety of arch dam can be judged by analyzing the change characteristics of extracted trend component.

### 4.1 Multi-Resolution Analysis for Observed Deformation Data Series

Assume that  $f(t)$  is a quadratically integrable function,  $f(t) \in L^2(R)$ , and  $\psi(t)$  is the mother wavelet. The wavelet transform of  $f(t)$  can be expressed as follows.

$$W_f(a, b) = \frac{1}{\sqrt{|a|}} \int_{-\infty}^{+\infty} f(t) \psi\left(\frac{t-b}{a}\right) dt \quad (7)$$

where  $a$  and  $b$  are the translation factor and the shrinkage factor, respectively;  $\psi_{ab}(t) = \frac{1}{\sqrt{|a|}} \psi\left(\frac{t-b}{a}\right)$  is a family of wavelet functions deduced from the elementary function  $\psi(\bullet)$  by translations and dilatations.

The function  $\psi(t)$  needs to satisfy the admissibility condition as follows.

$$\int_{-\infty}^{+\infty} \frac{|\psi(\omega)|^2}{|\omega|} d\omega < +\infty \quad (8)$$

where  $\psi(\omega) = \int_{-\infty}^{+\infty} \psi(t) e^{-i\omega t} dt$  represents the Fourier transform.

The function  $\psi(\omega)$  needs to have a band-pass property and enough quick attenuation. The function  $\psi(t)$  needs to have a vibration waveform alternating in a positive and negative way, and its mean is zero, namely

$$\int_{-\infty}^{+\infty} \psi(t) dt = 0 \quad (9)$$

In practice, the signal is often obtained with a certain time interval. So it is necessary to implement the wavelet base discretization for analyzing the actual signal. Generally,  $a = 2^j$ ,  $b = 2^j k$ , and  $j$  and  $k$  are all integers.



Multi-resolution analysis in the space  $L^2(R)$  means that there is a closed subspace  $\{V_j\}_{j \in Z}$  in  $L^2(R)$ , which satisfies the following properties (Seo et al. 2015; Wang et al. 2009).

- (1) Monotonicity.  $V_j \subset V_{j+1}$  for any of  $j \in Z$ .
- (2) Approximation.  $\bigcup_{j=-\infty}^{+\infty} V_j = L^2$  and  $\bigcap_{j=-\infty}^{+\infty} V_j = \{0\}$  for any of  $j \in Z$ .
- (3) Scalability.  $f(t) \in V_j \Leftrightarrow f(2t) \in V_{j+1}$ .
- (4) Translation invariance.  $\varphi\left(2^{\frac{j}{2}}t\right) \in V_j \Leftrightarrow \varphi\left(2^{\frac{j}{2}}t-k\right) \in V_j$  for any of  $k \in Z$ .
- (5) Riesz base existence. There is a function vector  $\varphi(x) \in V_0$  that makes  $\left\{2^{\frac{j}{2}}\varphi\left(2^{\frac{j}{2}}x-k\right), k \in Z\right\}$  be the Riesz base of  $V_j$ .

Assume that  $W_j$  is the orthogonal complement space of  $V_j$  in  $V_{j+1}$ , namely  $V_{j+1} = V_j \oplus W_j$  and there is a functional vector  $\varphi(x)$  making  $\left\{2^{\frac{j}{2}}\varphi\left(2^{\frac{j}{2}}x-k\right), k \in Z\right\}$  be the orthonormal base in  $W_j$ . Thus  $\varphi_{j,n}(x) = 2^{\frac{j}{2}}\varphi\left(2^{\frac{j}{2}}x-k\right)$ . Assume that  $V_j$  is the decomposed low-frequency part  $A_j$  and  $W_j$  is the decomposed high-frequency part. Then  $W_j$  is the orthogonal complement of  $V_j$  in  $V_{j+1}$ , namely  $V_j \oplus W_j = V_{j+1}$ .

$$V_j \oplus W_j \oplus W_{j+1} \oplus \dots \oplus W_{j+m} = V_{j+m} \tag{10}$$

Thus, the subspace  $V_0$  of multi-resolution analysis can be approximated with the finite subspaces, namely

$$V_0 = V_1 \oplus W_1 = V_2 \oplus W_2 \oplus W_1 = \dots = V_N \oplus W_N \oplus W_{N-1} \oplus \dots \oplus W_2 \oplus W_1 \tag{11}$$

It can be obtained from above multi-resolution analysis that  $L^2(R) = \sum_{j=-\infty}^s W_j \oplus V_s$ , where  $s$  is an arbitrary scale. The following wavelet expansions can be obtained by expanding the signals  $f(t) \in L^2(R)$  in the space  $L^2(R)$ .

$$f(t) = \sum_{k \in Z} a_k^s \varphi_{J,k}(t) + \sum_{j \leq s} \sum_{k \in Z} d_k^j \psi_{j,k}(t) \tag{12}$$

where the first item is the low-frequency part on the scale  $s$ ; the second item is the high-frequency part on the decomposition scales;  $a_k^s$  and  $d_k^j$  are the coefficients of wavelet transformation.

### 4.2 Trend Component Extraction and Safety Criterion of Arch Dam Deformation

The observations of arch dam deformation can be regarded as a digital signal series composed of the components with different frequencies. The observed deformation data are influenced by environmental factors, observation errors, other random factors. The deformation component influenced by the periodic environmental factors has the obvious seasonal variation characteristics with higher frequency. The deformation component, which is influenced by the observation errors and other random factors, fluctuates with high frequency and short cycle. The trend component of dam deformation changes with low frequency and long cycle.

Assume that  $X(t)$  represents an observed deformation data series of arch dam. The multi-layer wavelet decomposition formula as Eq. (12) is taken to decompose the series  $X(t)$ . The follows can be obtained.

$$X(t) = A + D \quad (13)$$

where  $A = \sum_{k \in Z} a_k^s \varphi_{J,k}(t)$  denotes the change with low frequency and long cycle for the observed deformation data series of arch dam;  $D = \sum_{j \leq s} \sum_{k \in Z} d_k^j \psi_{j,k}(t)$  denotes the change with high or higher frequency and short cycle for the observed deformation data series.

The following quadratic curve is used to fit the development process of trend component on arch dam deformation.

$$f_\theta = a_0 + a_1 t + a_2 t^2 \quad (14)$$

The following approximation can be obtained.

$$f_\theta = a_0 + a_1 t + a_2 t^2 \quad (15)$$

The first-order and second-order derivatives of Eq. (15) are derived as follows.

$$\frac{df_\theta}{dt} = a_1 + 2a_2 t \quad (16)$$

$$\frac{d^2 f_\theta}{dt^2} = 2a_2 \quad (17)$$

From Eqs. (16–17), it is easy to analyze the development of trend components, and then identify the deformation safety of arch dam. If  $a_2 < 0$ , the variation trend of dam deformation is normal. If  $a_2 = 0$ , the variation trend of dam deformation is abnormal. If  $a_2 > 0$ , the variation trend of dam deformation is dangerous. The deformation status of arch dam can be diagnosed comprehensively by combining the variation trend with the multi-level control value.

## 5 Example Analysis

One actual arch dam is taken as an example. According to the analyzed results on observed data of horizontal displacement and the structural calculations with FEM, the proposed criterion and approach are used to determine the early-warning index on dam deformation. The deformation behavior of arch dam is identified.

### 5.1 Engineering Overview and Dam Deformation Observation

A hydropower station is located on the upper Yellow River in China. The construction officially began in April 1988, the storage water began in December 1996, and the first unit was put into operation in April 1999. The whole project was fulfilled in December 2001. The

check flood level, the design flood level, the normal storage water level, the flood control level and the dead water level are 2182.6 m, 2181.3 m, 2180.0 m, 2180.0 m and 2178.0 m respectively. The check reservoir storage and the normal reservoir storage are  $17.5 \times 10^8 \text{ m}^3$  and  $16.5 \times 10^8 \text{ m}^3$  respectively. The flood control capacity and the regulated storage capacity are  $1.6 \times 10^8 \text{ m}^3$  and  $0.6 \times 10^8 \text{ m}^3$  respectively.

As shown in Fig. 2, the key water-control project consists of the double curvature concrete arch dam with three circle centers, the left bank gravity pier, the left bank auxiliary gravity dam, the outlet structure and the powerhouse located at the dam toe. The concrete arch dam has a front length of 438.417 m and a dam crest axis length of 414 m. It is composed of 20 dam sections which are numbered 1–20 from right bank to left bank. The elevation of dam foundation surface is 2030 m and the elevation of dam crest is 2185 m. The maximum dam height is 155 m and the maximum base width is 45 m. The three left bank gravity piers with a length of 56.98 m, a maximum height of 28.5 m and a crest elevation of 2187.5 m, are located above the elevation of 2157 m. The gravity piers are numbered G1–G3, and are connected with No. 20 arch dam section. The left bank auxiliary gravity dam with a crest length of 100 m, a maximum height of 32.5 m and a crest elevation of 2187.5 m is connected with the gravity pier.

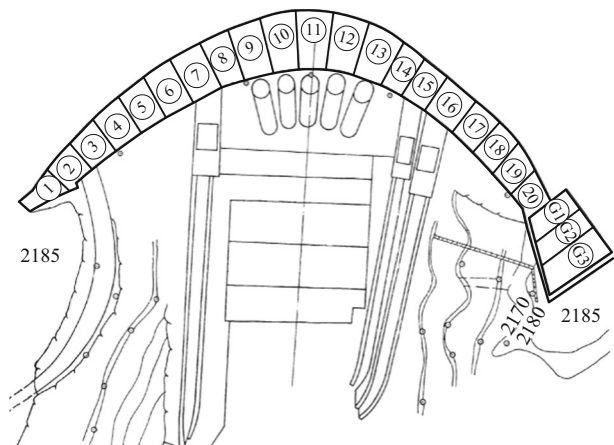
The pendulum lines were installed to measure the horizontal displacement. As shown in Fig. 3, there are 7 groups of pendulum lines with 32 monitoring points, which are placed in No. 11 dam section at the arch crown, Nos. 6 and 16 dam sections at 1/4 arches of left and right banks, No. 1 dam section, Nos. G1 and G3 dam section at arch abutments, and the right bank foundation.

The monitoring points with the great change of observed data, which are placed in the crown cantilever, are generally taken as representative points to determine the early-warning index of arch dam deformation. In this paper, the monitoring point, which is located at the elevation of 2185 m in No. 11 dam section, is selected.

## 5.2 Multi-Level Control Value Determination of Dam Deformation

The strength, stability and crack are regarded as main constraint conditions. The strength reduction-based FEM is adopted to calculate the global safety factor of arch dam and determine the control values of arch dam deformation.

**Fig. 2** General layout of key water-control project



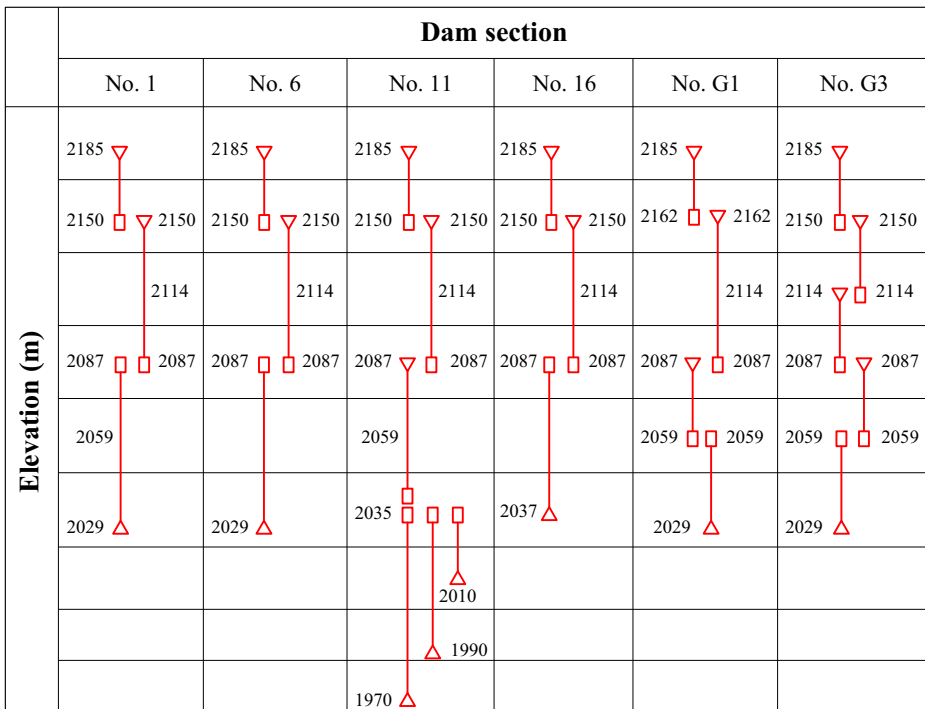


Fig. 3 Pendulum line layout

### 5.2.1 Calculation Scheme of FEM

In the FEM calculation, the normal storage water level is taken as the hydraulic load and the temperature load is calculated with the measured temperature data. The Drucker-Prage yield criterion-based constitutive model is adopted in dam body and dam foundation. It can be known by analyzing the observed data of dam body temperature that the lowest and highest temperatures in dam body appear in early March and September respectively. So the differences between the joint closure temperature and the measured temperatures on March 10, 2003, September 10, 2003 are regarded as the temperature drop load and temperature rise load, respectively. The measured joint closure temperatures are listed in Table 1.

It can be known from the FEM calculation under the action of temperature drop and temperature rise that the maximal displacement of crown cantilever section occurs in the temperature drop period. So the temperature drop is taken as a control case of arch dam stability. In the FEM calculation process, the strength reduction coefficient increases gradually from 1. The displacement field of arch dam under different strength conditions can be obtained by inputting the reduced material strength parameters into the finite element model.

The finite element model of arch dam, as shown in Fig. 4, is built as follows. The upstream dam foundation is taken 1 times of dam height (about 150 m). The left and right abutment rock masses are taken 1 times of dam height (about 150 m). The downstream dam foundation is taken 2 times of dam height (about 300 m). The depth of dam foundation is taken 1.5 times of dam height (about 200 m). The main boundary scope, which may affect the FEM calculation results, are considered in the finite element model. The geometric shape of dam body and the rock layer partition of dam foundation are simulated. Besides, the model also simulates the

**Table 1** Average measured joint closure temperatures of all dam sections

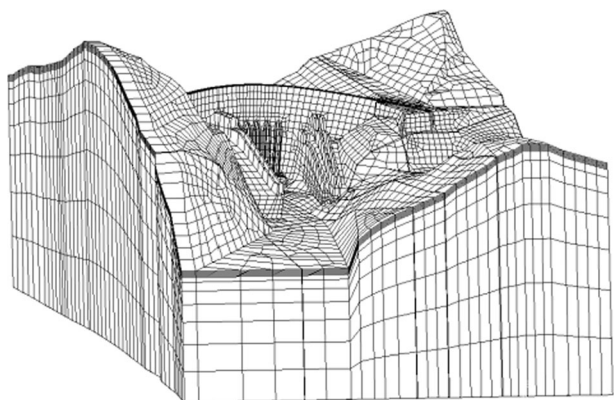
Elevation (m)	Temperature of dam section (°C)		Elevation (m)	Temperature of dam section (°C)	
	Nos. 9–13	Nos. 1–8, 14–20		Nos. 9–13	Nos. 1–8, 14–20
2030.5–2038.8	9.8	8.4	2104.5–2113.5	6.4	7.2
2038.8–2046.5	11.2	6.7	2113.5–2124.5	6.2	7.8
2046.5–2054.5	10.3	8.5	2124.5–2134.5	6.2	8.3
2054.5–2062.5	8.5	7.6	2134.5–2144.5	5.3	8.0
2062.5–2070.5	7.8	7.2	2144.5–2154.5	6.5	8.2
2070.5–2078.5	7.0	7.3	2154.5–2164.5	6.5	7.1
2078.5–2086.5	6.7	7.9	2164.5–2174.5	6.0	6.5
2086.5–2094.5	6.3	7.5	2174.5–2184.5	4.9	6.6
2094.5–2104.5	6.9	8.1			

drainage holes, the foundation concrete, the dam back tube and the town piers at the elevation of 2059 m. An eight-node hexahedral isoparametric element is taken as the main finite-element type, and a few six-node pentahedral isoparametric elements are used. The model is made up 46,883 elements and 50,516 nodes.

The dam body and dam foundation are divided into different material areas. At the same time, the dam concrete and the dam foundation rock are both regarded as isotropic material. The distribution of elastic modulus in the dam foundation is in Fig. 5. Other initial material parameters of dam body and dam foundation with faults, which are used in the calculation, are listed in Table 2.

### 5.2.2 Displacement Analysis of Characteristic Points

In this paper, the plastic zone run-through criterion of structural planes and the displacement jump criterion of characteristic points are combined to evaluate the global stability of arch dam. So the characteristic points, which are very sensitive to the arch dam deformation, need be selected (Li et al. 2009; Su et al. 2016). The sensitivities of the deformations at the different elevations in dam body on the elastic moduli are analyzed to determine the characteristic points. In order to simplify the calculation, the elastic modulus partition is generalized, as shown in Fig. 6. The selected parameters are  $E_{r1}$  corresponding with A-type rock mass,  $E_{r2}$

**Fig. 4** Finite element model

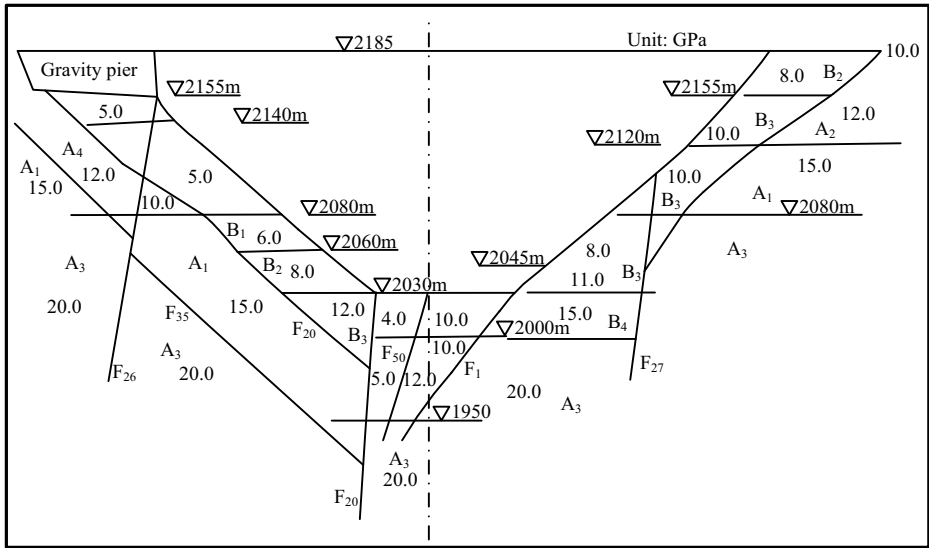


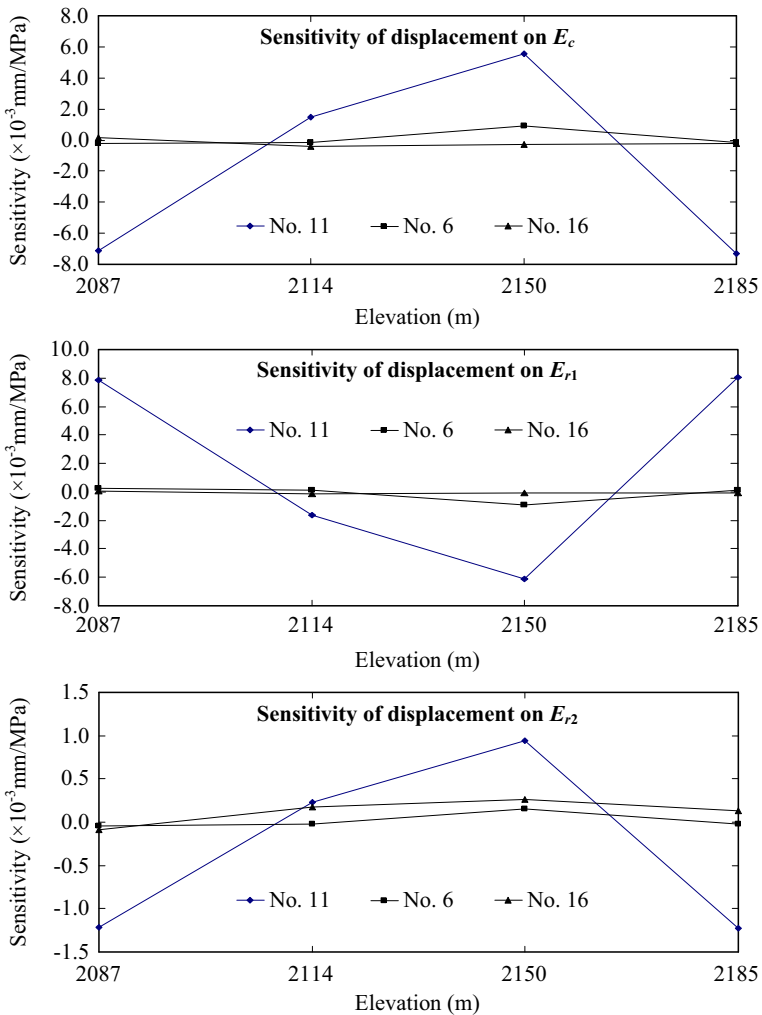
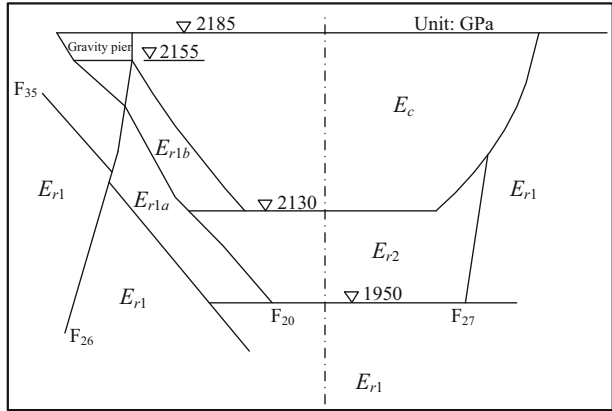
**Fig. 5** Elastic modulus distribution in dam foundation with faults

corresponding with B-type rock mass and  $E_c$  corresponding with dam body concrete. Besides,  $E_{r1a} = 0.75E_{r1}$ ,  $E_{r1b} = 0.5E_{r1}$ . The sensitivities of dam body displacements on elastic moduli ( $E_c$ ,  $E_{r1}$ ,  $E_{r2}$ ) are calculated. The calculated sensitivities are shown in Fig. 7.

**Table 2** Initial material parameters of dam body and dam foundation with faults

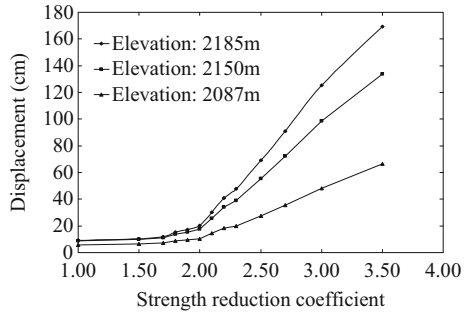
Location	Elastic modulus (GPa)	Poisson's ratio	Density (kg/m <sup>3</sup> )	Linear expansion coefficient (°C <sup>-1</sup> )	Friction coefficient	Cohesion (MPa)
Dam body concrete	20	0.167	2400	$1 \times 10^{-5}$	1.0	2.5
Dam foundation A <sub>1</sub>	15	0.2	2850	$1 \times 10^{-5}$	1.2	2.0
Dam foundation A <sub>2</sub>	20	0.2	2850	$1 \times 10^{-5}$	1.2	2.0
Dam foundation A <sub>4</sub>	12	0.2	2850	$1 \times 10^{-5}$	1.2	2.0
Dam foundation B <sub>1</sub>	6.0	0.23	2750	$1 \times 10^{-5}$	0.75	0.75
Dam foundation B <sub>2</sub>	8.0	0.23	2750	$1 \times 10^{-5}$	0.8	0.9
Dam foundation B <sub>3</sub>	10	0.23	2750	$1 \times 10^{-5}$	0.85	1.0
Dam foundation B <sub>4</sub>	12	0.23	2750	$1 \times 10^{-5}$	1.2	2.0
Fault F <sub>26</sub>	2.0	0.35	1950	$1 \times 10^{-5}$	0.35	0.01
Fault F <sub>27</sub>	2.0	0.35	1950	$1 \times 10^{-5}$	0.35	0.01
Fault F <sub>20</sub>	2.0	0.35	1950	$1 \times 10^{-5}$	0.35	0.01
Fault F <sub>50</sub>	2.0	0.35	1950	$1 \times 10^{-5}$	0.35	0.01
Fault F <sub>35</sub>	2.0	0.35	1950	$1 \times 10^{-5}$	0.35	0.01

**Fig. 6** Generalized partition of elastic modulus



**Fig. 7** Displacement sensitivities of three dam sections on elastic moduli

**Fig. 8** Relationship curve between the displacement at characteristic elevation and the strength reduction coefficient



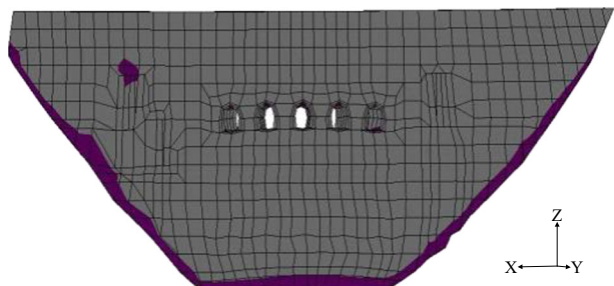
It can be seen from Fig. 7 that the absolute sensitivity of No. 11 dam section is larger. It is indicated that the tiny deformation of No. 11 dam section is enough to cause the remarkable parameter fluctuation. The sensitivities of Nos. 6 and 16 dam sections are near zero. The smaller values means that the deformation variations of Nos. 6 and 16 dam sections are lowly sensitive to the material parameter. It can be further seen that for No. 11 dam section, the sensitivity at the elevation of 2114 m is smaller and is near zero. So the monitoring points at the elevations of 2087 m, 2150 m and 2185 m in No. 11 dam section are taken as the characteristic points for evaluating the global stability of arch dam.

Fig. 8 shows the relationship curve between the characteristic point displacement and the strength reduction coefficient. It can be seen from Fig. 8 that the dam deformation can be mainly divided into three phase with two breaking points on the relationship curve, namely the linear elastic phase, the elastoplastic phase and the instability failure phase. As shown in Fig. 8, the dam is in a linear elastic phase before the strength reduction coefficient reaches 1.7. The dam is stable before the strength reduction coefficient reaches 2.0. The dam displacement jump appears when the strength reduction coefficient reaches 2.0 and the non-convergence of calculation emerges with the increase of reduction coefficient. So it can be considered that the global stability safety factor of arch dam is about 2.0.

### 5.2.3 Control Value Determination of Dam Deformation

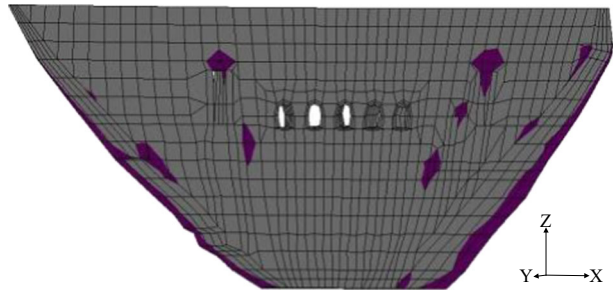
For one arch dam, the instability failure is not allowable in service. So the third-level control value of dam deformation needs be determined only for some special projects. In this paper, the monitoring point, which is located at the elevation of 2185 m in No. 11 dam section, is taken as an example. Its first-level and second-level control values

**Fig. 9** Plastic zone distribution on upstream surface of dam body when reduction coefficient is 1.7





**Fig. 10** Plastic zone distribution on downstream surface of dam body when reduction coefficient is 1.7



are investigated. The elastoplastic constitutive model is used in the FEM calculation. The calculating condition is the normal storage water level of 2180.0 m with the maximum rise and drop of temperature. It can be known from the FEM calculation that the maximal dam displacements at the different elevations occur in the temperature drop period. So the temperature drop is a control case.

- (1) The first-level control value estimation of dam deformation. It can be known from the FEM calculation under the action of normal storage water level load that the stress at any location in dam body does not exceed the proportional limit of material strength. The tensile principal stress and the compressive principal stress of arch dam satisfy the stress control standard. So the arch dam is stable and safe under the normal storage water level condition. It can be known from the strength reduction-based calculation that the stress and strain are in the linear elastic or quasilinear elastic range when the reduction coefficient is less than 1.7.

Figs. 9, 10, 11 show the plastic zone distribution of arch dam when the reduction coefficient reaches 1.7. It can be seen from Figs. 9, 10, 11 that the dam heel and the upstream arch abutment have been yielded. The plastic zone appears in the downstream surface near the drain hole after the stress redistribution. When the reduction coefficient reaches 1.7, the dam foundation surface at dam heel has been yielded but a run-through yield region does not be formed. Therefore, according to the comprehensive analysis for the plastic zone in the dam body and the dam foundation surface, it can be considered that the dam is in an elastic working stage when the reduction coefficient is 1.7.

It can be known from the FEM calculation that the maximal radial displacement of arch dam appears at the crown cantilever crest. So the displacement control value at

**Fig. 11** Plastic zone distribution on dam foundation surface when reduction coefficient is 1.7

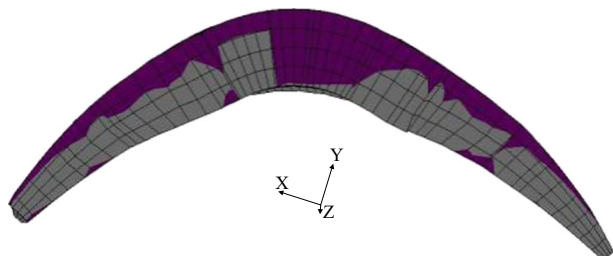
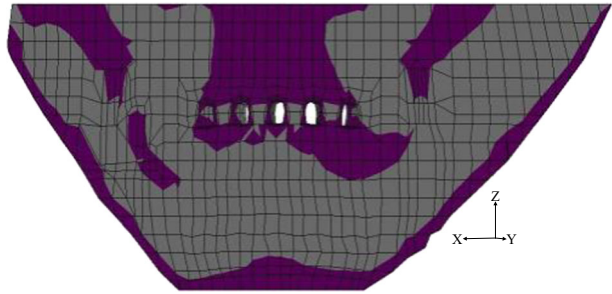


**Fig. 12** Plastic zone distribution on upstream surface of dam body when reduction coefficient is 2.0



the crown cantilever crest is determined. The maximal radial displacement of dam crest in an elastic working stage is 11.79 cm. The displacement control value can be estimated as follows.

$$\delta_{1m} = (11.79 - 0.271\theta - 0.497\ln\theta) \text{ cm} \quad (18)$$

where  $\theta = t/100$ ,  $t$  represents the cumulative days between the current monitoring time and the beginning monitoring time in the observed displacement data series.

- (2) The second-level control value estimation of dam deformation. It can be seen from Fig. 8 that the change of dam displacement is nonlinear when the strength reduction coefficient is between 1.7 and 2.0. The arch dam is in an elastoplastic stage. Figs. 12, 13, 14 show the plastic zone distribution of arch dam when the reduction coefficient reaches 2.0.

It can be seen from Figs. 9, 10, 11, 12, 13, 14 that with the change of material parameters in dam body, the crack zone and the plastic yield zone in dam body expand gradually, the downstream compressive stress of arch dam increases. The run-through yield regions in dam bottom, left and right upstream abutments have been basically formed. A wide range of yield zone is formed in downstream dam abutment. A large area of yield appears on the upstream surface of dam body near the diversion hole, especially at the junction of arch dam body and gravity pier. At the same time, the weak structural plane in dam foundation slips locally and the dam displacement increases nonlinearly. It is obvious that the run-through plastic region have been

**Fig. 13** Plastic zone distribution on downstream surface of dam body when reduction coefficient is 2.0

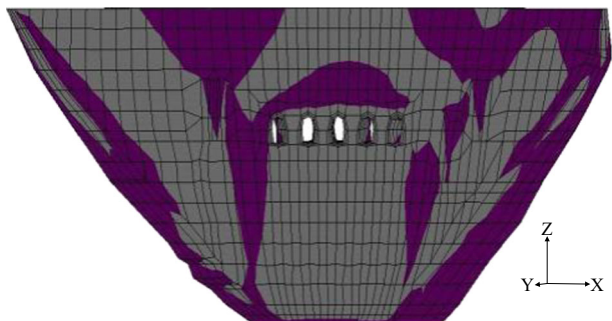
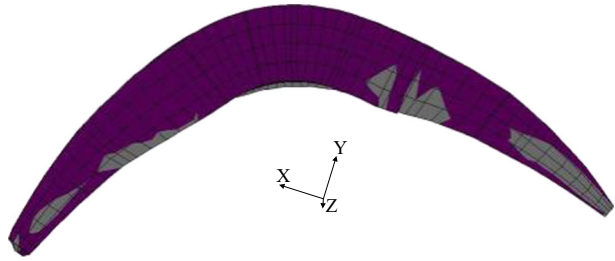


**Fig. 14** Plastic zone distribution on dam foundation surface when reduction coefficient is 2.0



formed on the dam foundation surface. Therefore, according to the comprehensive analysis for the plastic zone in the dam body and the dam foundation surface, it can be considered that the dam is in a yield deformation working stage when the reduction coefficient is 2.0. After the strength reduction coefficient is greater than 2.0, the crack range of arch dam extends widely, the zones of yield and compression failure expand quickly. It can be judged that the arch dam has entered into the instability failure stage.

It can be known from the FEM calculation that with the continuous reduction of material strength in dam body and dam foundation, the displacement jump of crown cantilever appears when the strength reduction coefficient reaches 2.0. At this time, the maximal radial displacement at crown cantilever crest is 20.42 cm. So the radial displacement control value of dam crest can be estimated as follows.

$$\delta_{2m} = (20.42 - 0.271\theta - 0.497\ln\theta) \text{ cm} \tag{19}$$

where  $\theta = t/100$ ,  $t$  represents the cumulative days between the current monitoring time and the beginning monitoring time in the observed displacement data series.

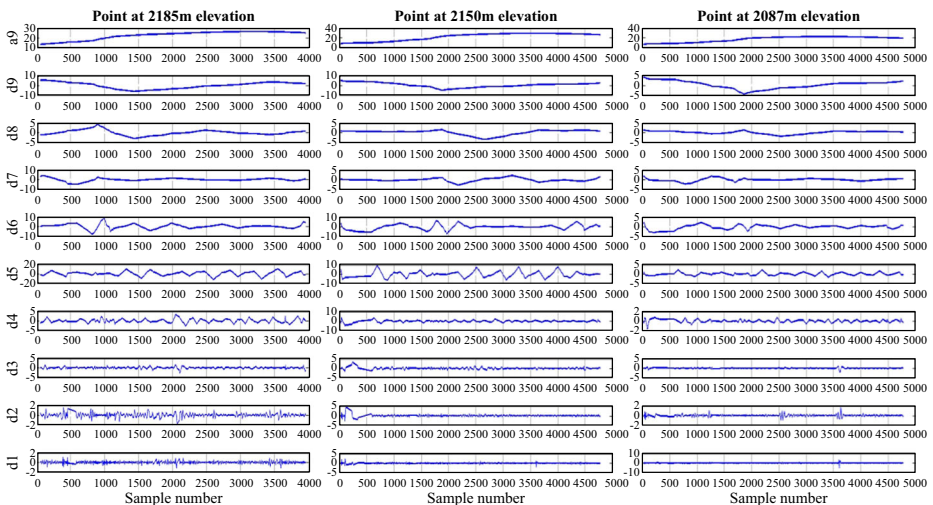


**Fig. 15** Wavelet decomposition results for monitoring points at the elevations of 2087 m, 2150 m and 2185 m

### 5.3 Trend Analysis and Safety Evaluation of Dam Deformation

The radial displacements of three monitoring points at the elevations of 2087 m, 2150 m and 2185 m in No. 11 dam section are taken as an example. Their variation trends are analyzed. The “db6” wavelet is adopted to implement the nine layers of decomposition for observed displacement data series. The result is shown in Fig. 15, where d1-d9 are the high-frequency parts of the first to ninth layer, a9 is the low-frequency part of the ninth layer.

It can be seen from Fig. 15 that the development trend of horizontal displacement data series gradually become obvious with the increase of decomposition scale and the decrease of corresponding time resolution. When the decomposition reaches the ninth layer, the high-frequency information, namely d1-d9, is filtered, the remained a9 is the trend component on horizontal displacement of arch dam. The quadratic polynomial is used to fit the trend component a9. Eqs. (20–22) give the fitting results for the three monitoring points at the elevations of 2087 m, 2150 m and 2185 m in No. 11 dam section.

$$\text{Monitoring point at the elevation of 2185 m : } y = 11.4 + 9.73 \times 10^{-3}t - 1.57 \times 10^{-6}t^2 \quad (20)$$

$$\text{Monitoring point at the elevation of 2150 m : } y = 3.25 + 1.32 \times 10^{-2}t - 1.69 \times 10^{-6}t^2 \quad (21)$$

$$\text{Monitoring point at the elevation of 2087 m : } y = 0.57 + 6.38 \times 10^{-3}t - 1.89 \times 10^{-6}t^2 \quad (22)$$

It can be seen from Fig. 15 and Eqs. (20–22) that  $d\delta_\theta/dt \neq 0$  and  $d^2\delta_\theta/dt^2 < 0$ , which indicates that the trend component of arch dam displacement increases with the decreasing rate and shows the convergence trend. At the same time, if the hidden dangers are not detected, it can be considered that the deformation behavior of arch dam is normal.

## 6 Conclusions

The early-warning index of structural response under the load combinations can be determined by analyzing the capacity bearing the past loads and then estimating the capacity bearing the future possible loads for one dam body-foundation system. The reasonable index can play an important role in identifying the service safety of dam engineering. The early-warning problem on arch dam deformation is investigated in this paper. An early-warning criterion combining the control value with the variation trend of dam deformation is built. The approaches determining the early-warning indices of arch dam deformation, namely the control value and the trend component, are developed by analyzing the prototypical observations of dam safety and implementing the numerical simulation of dam structure.

The control value of arch dam deformation is related to the failure process of arch dam. The deformation control values with three levels are determined by calculating the global safety factors of arch dam in different working stages. The observed deformation of arch dam is regarded as a signal with different frequencies. The trend component of arch dam deformation is extracted by implementing the wavelet multi-resolution analysis for observed deformation data series.

**Acknowledgements** This research has been partially supported by National Natural Science Foundation of China (SN: 51579083, 51479054, 41323001), the National Key Research and Development Program of China (SN: 2016YFC0401601), the Doctoral Program of Higher Education of China (SN: 20130094110010), Open Foundation of State Key Laboratory of Hydrology-Water Resources and Hydraulic Engineering (SN: 20165042112, 20145027612), the Fundamental Research Funds for the Central Universities (Grant No. 2015B25414).

## References

- Ardito R, Maier G, Massalongo G (2008) Diagnostic analysis of concrete dams based on seasonal hydrostatic loading. *Eng Struct* 30:3176–3185
- Cheng L, Zheng DJ (2013) Two online dam safety monitoring models based on the process of extracting environmental effect. *Adv Eng Softw* 57:48–56
- Jin F, Hu W, Pan JW, Jian Y, Wang JT, Zhang CH (2011) Comparative study procedure for the safety evaluation of high arch dams. *Comput Geotech* 38(3):306–317
- Hossain F (2010) Empirical relationship between large dams and the alteration in extreme precipitation. *Nat Hazards Rev* 11(3):97–101
- Huang M, Jia CQ (2009) Strength reduction FEM in stability analysis of soil slopes subjected to transient unsaturated seepage. *Comput Geotech* 36(1):93–101
- Kao CY, Loh CH (2013) Monitoring of long-term static deformation data of Fei-Tsui arch dam using artificial neural network-based approaches. *Struct Control Health Monit* 20:282–303
- Lei P, Chang XL, Xiao F, Zhang GJ, Su HZ (2011) Study on early warning index of spatial deformation for high concrete dam. *Sci China Ser E* 54(6):1607–1614
- Li X, Li Y, Chen DW (2009) Application of homotopy parameter inversion method in Miyun reservoir. *Global Geology* 12(2):109–111
- Lin P, Ma T, Liang Z, Tang CA, Wang R (2014) Failure and overall stability analysis on high arch dam based on DFPA code. *Eng Fail Anal* 45:164–184
- Mata J, Tavares de Castro A, Sá da Costa J (2014) Constructing statistical models for arch dam deformation. *Struct Control Health Monit* 21:423–437
- Ranković V, Grujović N, Divac D, Milivojević N (2014) Development of support vector regression identification model for prediction of dam structural behaviour. *Struct Saf* 48:33–39
- Seo Y, Kim S, Kisi O, Singh VP (2015) Daily water level forecasting using wavelet decomposition and artificial intelligence techniques. *J Hydrol* 520:224–243
- Stojanovic B, Milivojevic M, Ivanovic M, Milivojevic N, Divac D (2013) Adaptive system for dam behavior modeling based on linear regression and genetic algorithms. *Adv Eng Softw* 65:182–190
- Su HZ, Hu J, Wu ZR (2012) A study of safety evaluation and early-warning method for dam global behavior. *Struct Health Monit* 11(3):269–279
- Su HZ, Wen ZP, Sun XR, Yang M (2015) Time-varying identification model for dam behavior considering structural reinforcement. *Struct Saf* 57:1–7
- Su HZ, Wen ZP, Wu ZR (2011) Study on an intelligent inference engine in early-warning system of dam health. *Water Resour Manag* 25(6):1545–1563
- Su HZ, Wen ZP, Zhang S, Tian SG (2016) Method for choosing the optimal resource in back-analysis for multiple material parameters of a dam and its foundation. *J Comput Civ Eng* 30(4):04015060
- Sujatha V, Chandra Kishen JM (2003) Energy release rate due to friction at bimaterial interface in dams. *J Eng Mech* 129(7):225–230
- Wang W, Jin J, Li Y (2009) Prediction of inflow at three gorges dam in Yangtze River with wavelet network model. *Water Resour Manag* 23(13):2791–2803
- Wu ZR, Peng Y, Li ZC, Li B, Yu H, Zheng SR (2011) Commentary of research situation and innovation frontier in hydro-structure engineering science. *Sci China Ser E* 54(4):767–780
- Wu ZR, Su HZ (2005) Dam health diagnosis and evaluation. *Smart Mater Struct* 14(3):S130–S136
- Yenigun K, Erkek C (2007) Reliability in dams and the effects of spillway dimensions on risk levels. *Water Resour Manag* 21(4):747–760
- Zhong DH, Sun YF, Li MC (2011) Dam break threshold value and risk probability assessment for an earth dam. *Nat Hazards* 59(1):129–147